

CHEMISTRY

AN **ASIAN** JOURNAL

www.chemasianj.org

Accepted Article

Title: Doubly N-Confused Calix[6]phyrin Bis-Organopalladium Complexes: Photostable Triplet Sensitizers for Singlet Oxygen Generation

Authors: Poornenth Pushpanandan, Dong-Hoon Won, Shigeki Mori, Yuhsuke Yasutake, Susumu Fukatsu, Masatoshi Ishida, and Hiroyuki Furuta

This manuscript has been accepted after peer review and appears as an Accepted Article online prior to editing, proofing, and formal publication of the final Version of Record (VoR). This work is currently citable by using the Digital Object Identifier (DOI) given below. The VoR will be published online in Early View as soon as possible and may be different to this Accepted Article as a result of editing. Readers should obtain the VoR from the journal website shown below when it is published to ensure accuracy of information. The authors are responsible for the content of this Accepted Article.

To be cited as: *Chem. Asian J.* 10.1002/asia.201801671

Link to VoR: <http://dx.doi.org/10.1002/asia.201801671>

A Journal of



A sister journal of *Angewandte Chemie*
and *Chemistry* – A European Journal

WILEY-VCH

Doubly N-Confused Calix[6]phyrin Bis-Organopalladium Complexes: Photostable Triplet Sensitizers for Singlet Oxygen Generation

Poornenth Pushpanandan,^[a] Dong-Hoon Won,^[a] Shigeki Mori,^[b] Yuhsuke Yasutake,^[c] Susumu Fukatsu,^[c] Masatoshi Ishida,^{*[a]} and Hiroyuki Furuta^{*[a]}

Abstract: Triplet photosensitizers that generate singlet oxygen efficiently are attractive for applications such as photodynamic therapy (PDT). Extending the absorption band to a near-infrared (NIR) region (700 nm~) with reasonable photostability is one of the major demands in the rational design of such sensitizers. We herein prepared a series of mono- and bis-palladium complexes (**1-Pd-H₂**, **2-Pd-H₂**, **1-Pd-Pd**, and **2-Pd-Pd**) based on modified calix[6]phyrins as photosensitizers for singlet oxygen generation. These palladium complexes showed intense absorption profiles in the visible-to-NIR region (500–750 nm) depending on the number of central metals. Upon photoirradiation in the presence of 1,5-dihydroxynaphthalene (DHN) as a substrate for reactive oxygen species, the bis-palladium complexes generated singlet oxygen with high efficiency and excellent photostability. Singlet oxygen generation was confirmed from the characteristic spectral feature of the spin trapped complex in the EPR spectrum and the intact ¹O₂ emission at 1270 nm.

organic chromophores (e.g., BODIPYs)^[7], poly-pyridyl transition metal complexes (Pt^{II}, Ru^{II}, Ir^{III})^[8] and metallo-macrocyclic complexes with porphyrin/phthalocyanine scaffolds^[9] have gained much attention as they showed sufficient singlet oxygen generation capabilities. In order to attain the higher efficiency for singlet oxygen generation, 1) strong absorption (in the near-infrared (NIR) biological window for PDT), 2) photostability, 3) high triplet state quantum yields (effective intersystem crossing (ISC)), 4) reasonably long-lived triplet state lifetime, and 5) solubility in appropriate media, are essentially required for the photosensitizers. For this purpose, the porphyrin-based chromophores have some benefits; tunable photophysical properties (i.e., molecular orbital symmetries and energies) by facile modification of the parent frameworks and by changing the central metal cations in the macrocyclic ligand.^[10] Largely, the metal complexes show reasonable durability even under the strong photo-irradiation.

Introduction

Singlet oxygen (¹Δ_g) is the lowest excited electronic state of oxygen and is one of the most important reactive oxygen species (ROS) playing a key role in many photoinduced oxidative processes in biological/chemical systems.^[1] Generally, singlet oxygen can be generated by using molecular oxygen (³O₂) under UV illumination with triplet photosensitizers. The well accepted microscopic mechanism is such that, the characteristic species in the triplet state formed via intersystem crossing (ISC) from the photo-excited singlet state transfers the energy to ³O₂.^[2] Such photosensitizers are thus useful in many applications such as photodynamic therapy (PDT),^[3] oxygen sensing,^[4] photocatalysis,^[5] and triplet-triplet annihilation upconversion.^[6] To date, many triplet sensitizers, such as heavy-atom-substituted

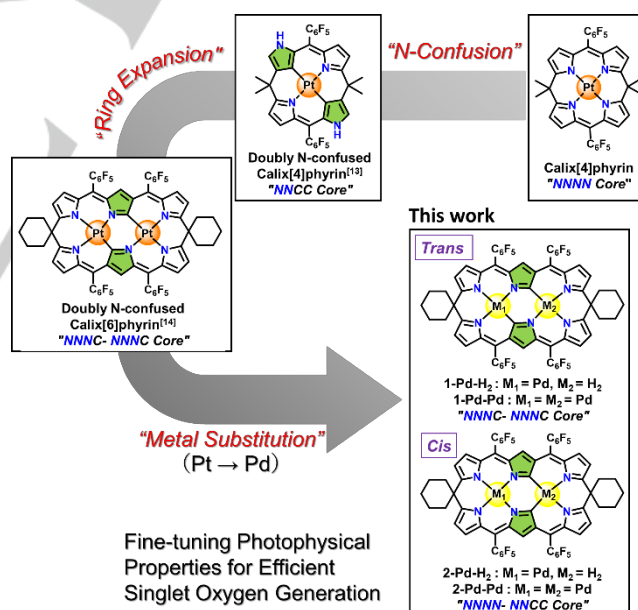


Figure 1. Strategic design of bis-Pd calix[6]phyrin complexes. Chemical structures of previously reported complexes, Pt-calix[4]phyrin, Pt-doubly N-confused calix[4]phyrin, bis-Pt calix[6]phyrin, and mono- and bis-Pd calix[6]phyrin complexes used in this work.

Calixphyrin is a unique class of the porphyrin analogues containing one or multiple *sp*³-hybridized *meso*-carbon bridges providing intrinsic molecular flexibility to endure facile cation bindings.^[11] From the interest of the effect of the carbon-metal

[a] P. Pushpanandan, Dr. D.-H. Won, Dr. M. Ishida, Prof. Dr. H. Furuta
 Department of Chemistry and Biochemistry
 Graduate School of Engineering and Center for Molecular Systems
 Kyushu University
 Fukuoka 819-0395 (Japan)

[b] Dr. S. Mori
 Advanced Research Support Center
 Ehime University
 Matsuyama 790-8577 (Japan)

[c] Dr. Y. Yasutake, Prof. Dr. S. Fukatsu
 Graduate School of Arts and Sciences
 The University of Tokyo
 Tokyo 153-8902 (Japan)

Supporting information and the ORCID identification number(s) for the author(s) of this article can be found under <https://doi.org/10.1002/asia.xxxxxxxx>.

FULL PAPER

bond in the macrocyclic core for photosensitizers, we have been working on the modified (confused) porphyrin and calix[4]phyrin(1.1.1.1) metal complexes.^[12,13] Despite the disrupted π -conjugation in the parent tetrapyrrolic scaffold, the NIR light absorption was achieved by electronic perturbation through an N-confusion modification of the platinum calix[4]phyrin complexes (Figure 1).^[13c] The doubly N-confused derivative demonstrated the lowest energy absorption and subsequently good singlet oxygen generation. Using this modification strategy, we have also reported novel NIR luminescent dyes based on doubly N-confused calix[6]phyrin(1.1.1.1.1.1) bis-platinum complexes.^[14] The core-expansion of the parent calix[4]phyrins induces the lower energy optical properties as there are more π -electrons in the scaffold. However due to the fact that the complexes possess relatively short triplet lifetimes (~ 15 ns) and insufficient triplet energy that could otherwise allow the energy transfer to dioxygen, the photosensitization for singlet oxygen generation remains yet to be achieved. Increasing the spin-orbit coupling decreases the triplet state life time and spin orbital coupling will increase with atomic number.^[15] Thus, we envisioned that replacing the platinum metal with palladium, in the row right above in the group 10 element column, should allow one to fine-tune the triplet state dynamics of the complexes. Moreover, the bis-palladium complex of doubly N-confused hexaphyrin exhibited a much lower energy absorption (~ 1470 nm) which should discourage energy transfer to singlet oxygen even though it has advantage in the absorption profile in the NIR region.^[16]

We herein report the facile synthesis of novel mono- and bis-palladium calix[6]phyrin complexes (**1-Pd-H₂**, **1-Pd-H₂**, **1-Pd-Pd**, and **2-Pd-Pd**) (Figure 1). The large π -conjugated scaffold based on the expanded calixphyrins attained prominent photophysical properties toward the NIR light region. The influence of the structural factors (e.g., coordination environment and the number of metal cations) on the photosensitized singlet oxygen generation were systematically investigated by X-ray

crystallographic analysis, NMR, absorption, emission, and EPR spectroscopies.

Results and Discussion

The synthetic route of the mono- and bis-palladium complexes, **1-Pd-H₂**, **2-Pd-H₂**, **1-Pd-Pd**, and **2-Pd-Pd**, is shown in the Scheme 1. The freebase calix[6]phyrin ligands (*transoid*, **1** and *cisoid*, **2**) were previously reported by our group, which serve as the rectangular-shaped macrocyclic ligands.^[14] The two isomeric macrocycles, **1** and **2**, in which the arrangement of the nitrogen atoms of the N-confused pyrrole rings (highlighted in green) is different, provide two organopalladium cation pockets surrounded by symmetrical and unsymmetrical coordination donor sites, "NNNC-NNNC" and "NNNN-NNCC", respectively. The corresponding bis-organopalladium metal complexes, **1-Pd-Pd** and **2-Pd-Pd**, were formed smoothly using 3 equivalents of Pd(OAc)₂ under reflux condition in a CH₂Cl₂/MeOH mixture, in 60 and 72% yields, respectively. Along with the formation of bis-palladium complexes, the mono-palladium complexes, **1-Pd-H₂** and **2-Pd-H₂**, were also formed in 30% and 22% yields, respectively. When one equivalent of Pd(OAc)₂ was added into the solution containing a ligand **1** or **2**, mono-palladium complex, **1-Pd-H₂** or **2-Pd-H₂** was predominantly obtained in 80 and 75% yields, respectively. The ¹H and ¹⁹F NMR spectroscopy and high-resolution mass spectrometry support the expected structures (*cf.* supporting information). Specifically, the complex **1-Pd-H₂** shows two characteristic signals at $\delta = 12.90$ (inner NH) and 10.59 ppm (inner CH) (Figure S1). However, the complex **2-Pd-H₂** shows one sharp inner CH signal at 10.26 ppm reflecting the molecular symmetry in the ¹H NMR spectrum (Figure S2). The symmetry of **1-Pd-H₂** is also reflected in the ¹⁹F NMR spectra; the splitting pattern of the *para*-substituted ¹⁹F signals of the peripheral aryl groups in a 1:2:1 ratio for **1-Pd-H₂** and a 2:1:1 ratio for **2-Pd-H₂**

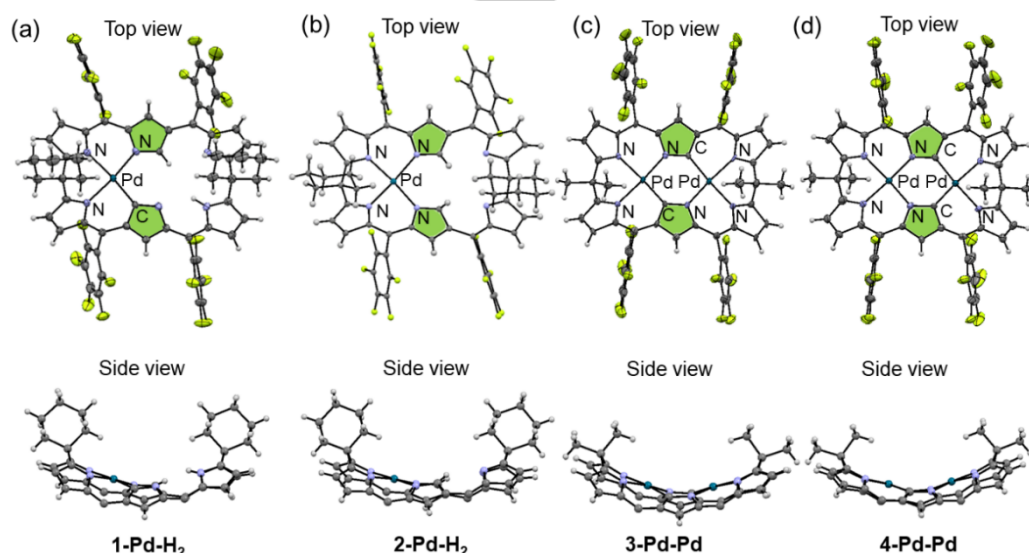
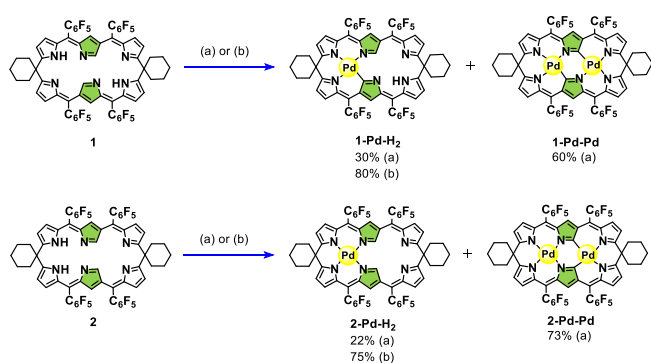


Figure 2. Top and side views of the X-ray crystal structures of (a) **1-Pd-H₂**, (b) **2-Pd-H₂**, (c) **3-Pd-Pd**, and (d) **4-Pd-Pd**. The confused rings are highlighted in green.

For internal use, please do not delete. Submitted_Manuscript

FULL PAPER



verifies their *trans/cis* configurations (Figures S1 and S2). These results suggested the porphyrin-like N₄ donor site in *cis*-configured **2** can preferentially accommodate a palladium cation before subsequent second palladium metalation occurs, to give **2-Pd-Pd**. The absence of the inner protons in the low field region (beyond 8 ppm) in the ¹H NMR spectra implies the successful bis-metalation in the core. The peripheral β-protons appear in the typical *sp*²-CH region due to the non-global π-conjugation as seen in the bis-platinum calixphyrin complexes.^[14]

The molecular structures of the complexes, **1-Pd-H₂**, **2-Pd-H₂**, **3-Pd-Pd**, and **4-Pd-Pd**, were characterized by X-ray crystallographic analysis (Figures 2 and S7, Table S1). The palladium cations reside in a square planar geometry in the inner coordination environments for all the complexes. The coplanar tripyrrin planes are faced with tethering *sp*³-hybridized *meso*-carbon centers located in the short axis side in the rectangular geometry. The overall core structures of the complexes exhibit bent-distortions along the longer molecular axis with the angles of 83–86°. The values for mean plane deviations (used with 36 core atoms) were estimated to be 0.717, 0.671, 0.743, and 0.770 Å for **1-Pd-H₂**, **2-Pd-H₂**, **3-Pd-Pd**, and **4-Pd-Pd**, respectively (Table S2). The formation of the organopalladium bonds may play an important role in the stabilization of the complexes as well as in the tuning of their electronic structures. Unfortunately, the disorder of the inner nitrogen versus adjacent carbon atoms of the confused pyrrole rings in the complexes hampered us to gain the discrete bonding information of the organopalladium complexes. The stronger bonding character of the Pd–C linkages than that of the Pd–N was speculated due to the intrinsic donor character of the anionic carbon sites.^[17] The theoretical structures of the complexes obtained from the density functional calculations reproduced the experimental structures (*vide infra*, Figure S8).

In order to study the optical properties of the complexes, UV-Vis-NIR spectra were recorded in toluene (Figure 3). All the complexes exhibit the intense absorption bands in the visible region ($\lambda_{\text{abs}} = 500\text{--}700\text{ nm}$) and tailing bands in the NIR region. The peak maxima of the mono-Pd complexes, **1-Pd-H₂** and **2-Pd-H₂**, appear around 560 nm ($\epsilon \sim 80000\text{ M}^{-1}\text{ cm}^{-1}$), whereas the peaks for the bis-Pd complexes, **1-Pd-Pd** and **2-Pd-Pd**, are seen in the lower energy region beyond 600 nm with relatively high absorption coefficient ($\epsilon \sim 90000\text{ M}^{-1}\text{ cm}^{-1}$) (Table 1). Interestingly,

depending on the molecular symmetry, the *trans*-configured complexes show relatively intense shoulder bands in the lower energy region.

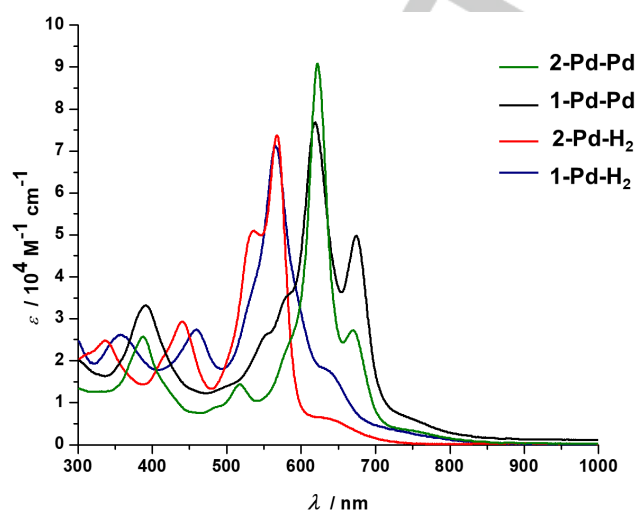


Figure 3. UV-vis-NIR absorption spectra of Pd complexes; **1-Pd-H₂** (blue line), **2-Pd-H₂** (red), **1-Pd-Pd** (black) and **2-Pd-Pd** (green) in toluene.

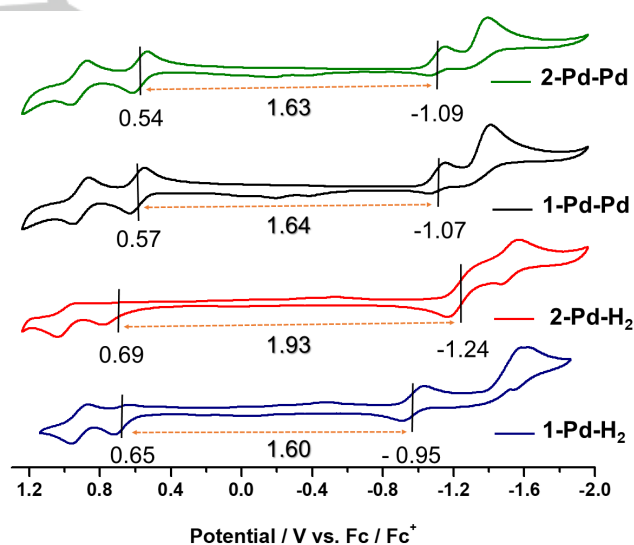


Figure 4. Cyclic voltammograms of **1-Pd-H₂**, **2-Pd-H₂**, **1-Pd-Pd**, and **2-Pd-Pd** in CH₂Cl₂ containing 0.1 M TBAPF₆. The scan rate is 100 mV s⁻¹, and the concentration was set to 1 mM.

Owing to the severely broadened absorption features in the NIR region, the HOMO-LUMO energy gap of the complexes was analyzed using cyclic voltammetry (CV) and differential pulse voltammetry (DPV) in dichloromethane containing 0.1 M tetrabutylammonium hexafluorophosphate (TBAPF₆) as the supporting electrolyte (Figures 4, S13, and S14). In fact, the bis-palladium complexes represent the similar redox profile: the quasi-reversible oxidation waves and irreversible reduction waves

For internal use, please do not delete. Submitted_Manuscript

FULL PAPER

were observed at $E_{ox} = 0.57$ and 0.54 V (vs ferrocene/ferrocenium couple) and $E_{red} = -1.07$ and -1.09 V, respectively. The corresponding energy gaps are thus calculated to be 1.64 and 1.63 V for **1-Pd-Pd** and **2-Pd-Pd**, respectively. In contrast, the irreversible oxidations at $E_{ox} = 0.65$ and 0.69 V, and the reduction at $E_{red} = -0.95$ and -1.24 V were observed for the mono-palladium complexes, **1-Pd-H₂** and **2-Pd-H₂**, respectively. The remarkably narrow HOMO-LUMO gap of **1-Pd-H₂** is originated from the anodic shift of the reduction wave than that of **2-Pd-H₂**, which implies the alteration of the electronic structures of the macrocycles.

In an effort to further elucidate the electronic structures of the complexes, density functional theory (DFT) calculations were carried out using B3LYP/6-31G**+SDD method. The π -electron present in the frontier molecular orbital diagrams was found to be delocalized over the π -ligands for all the complexes except for **1-Pd-H₂** (Figure S8). The LUMO pair of **1-Pd-H₂** indicated the partial localization on the tripyrrin moieties, which induces the broken-degeneracy of the LUMO/LUMO+1 pair. The feature in the remarkably stabilized LUMO causes the intrinsically narrower HOMO-LUMO gap of 2.07 V than that of the corresponding isomer **2-Pd-H₂** with the gap of 2.63 V. The surrounding metal-coordination environment can also contribute to the HOMO energy profiles; the palladium-carbon bonding nature within the NNNC sphere in **1-Pd-H₂** destabilizes the energy as reported for other porphyrinoids.^[18] The partial contribution from the d-orbital (d_{yz}) of organopalladium center in HOMO for **1-Pd-H₂** may influence the electronic alteration (but not for **2-Pd-H₂**). Similarly, the influence of metal d-electron in the ground state molecular orbitals for the organopalladium complexes was speculated through the Pd-C bond linkage. There is partial contribution from d-orbital in HOMO and HOMO-1, which should reflect to the optical properties.

The spectral features were analyzed using time-dependent (TD)-DFT calculations with B3LYP method (Figures S9–S12, Tables S3–S5). As discussed above, the *trans*-configured complexes, **1-Pd-H₂** and **1-Pd-Pd**, show intensified shoulder peaks compared to their *cis*-form counterparts, **2-Pd-H₂** and **2-Pd-Pd**, respectively. The TD-DFT calculations suggest that the transition from HOMO-1 to LUMO orbital contributes mostly and the oscillator strength of this transition is larger for the *trans*-form. Interestingly, partial MLCT contribution exists in the *trans*-forms

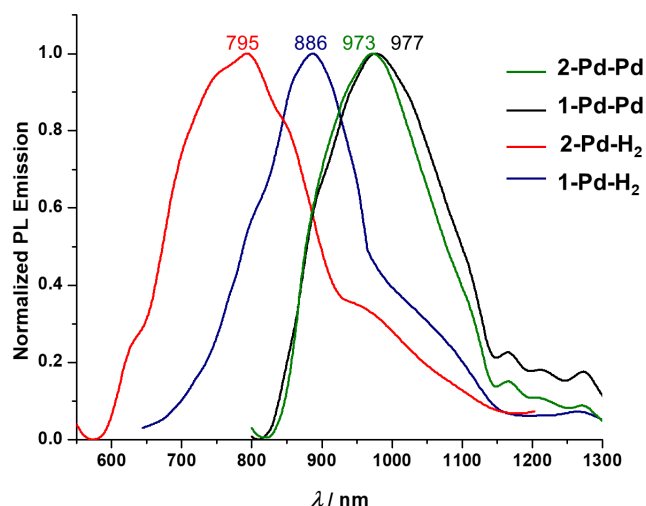


Figure 5. Phosphorescence spectra of **1-Pd-H₂**, **2-Pd-H₂**, **1-Pd-Pd**, and **2-Pd-Pd** in deaerated toluene at r.t. ($\lambda_{ex} = 532$ nm).

more than in the *cis*-form. Moreover, calculations also suggest the bathochromic shifts for bis-palladium complexes. As is the case with bis-platinum calix[6]phyrin complexes ($\lambda_{em} \sim 1020$ nm), a series of the palladium complexes indeed showed phosphorescence in the NIR region at room temperature in deaerated toluene (Figure 5 and Table 1). In terms of the energies, the bis-Pd complexes showed similar spectral feature ($E \sim 1.27$ eV). In contrast, the mono-Pd complexes indicated the varied emission energies in the order, **2-Pd-H₂** (1.56 eV) > **1-Pd-H₂** (1.40 eV) depending on the molecular symmetry.

The phosphorescence quantum yields and lifetimes of the series of complexes were determined to analyze the triplet state behaviors (Figures S15–S18). The phosphorescence lifetimes of bis-palladium complexes, **1-Pd-Pd** and **2-Pd-Pd**, are determined to be 183 and 174 ns, respectively, which are significantly larger than the photoluminescent lifetimes of Pt-calix[6]phyrin complexes (20–30 ns).^[14] In the case of the mono-palladium complexes, there is an apparent difference between the isomers; **2-Pd-H₂** possesses a significantly longer triplet state lifetime of 536 ns, whereas **1-Pd-H₂** has a short lifetime in the sub-microsecond time scale. In this regard, the phosphorescence quantum yields of **2-Pd-H₂** ($\Phi_{PL} = 3.9 \times 10^{-3}$) is significantly larger

Table 1. Summary of the photophysical parameters for the palladium complexes.

Complex	λ_{abs} (nm) ($\epsilon / 10^4 \text{ M}^{-1} \text{ cm}^{-1}$)	λ_{em} (nm)	$\Phi_{PL}^{[a]}$ (1×10^{-3})	τ_{PL} (ns) ^[b]	k_r (10^3 s^{-1})	k_{nr} (10^6 s^{-1})	$\Phi_{\Delta}^{[c]}$
1-Pd-H₂	566 (7.11)	886	0.56	127	4.4	7.8	0.05
2-Pd-H₂	568 (6.29)	795	3.9	536	7.3	1.8	0.83
1-Pd-Pd	619 (7.67)	977	1.2	183	6.5	5.4	0.30
2-Pd-Pd	622 (9.07)	973	2.1	174	11.9	5.7	0.27

^[a] Quantum yield was calculated using **4-Pt-Pt** ($\Phi_{PL} = 0.0027$ in toluene, $\lambda_{ex} = 532$ nm) as reference [14]. ^[b] Determined by TCSPC method with excitation at 532 nm. ^[c] Singlet oxygen quantum yield measured in $\text{CH}_2\text{Cl}_2/\text{MeOH}$ with methylene blue as standard.^[19]

For internal use, please do not delete. Submitted_Manuscript

FULL PAPER

than that of **1-Pd-H₂**. In the decay process, excited-state intramolecular proton transfer (ESIPT) of the pyrrolic NH moiety with adjacent pyrrole imine could be attributed for **1-Pd-H₂**. In contrast, the intrinsic strong C–H bonding nature of the N-confused pyrrole ring in **2-Pd-H₂** could have hindered this process.^[20] In the case of **1-Pd-Pd** and **2-Pd-Pd**, slightly smaller values of Φ_{PL} than that of **2-Pd-H₂** were obtained for both the bis-palladium complexes, probably due to the smaller energy gap.^[21] It is noteworthy that the *cis*-isomer was more luminescent than the *trans*-isomer as observed for bis-platinum complexes,^[14] although a further study is necessary to clarify the effect of the symmetrical/asymmetrical coordination environments on the excited states dynamics.

The emission due to the singlet oxygen ($^1\Delta_g$) was observed at 1270 nm from the solution of the palladium complexes during the phosphorescence measurements under the aerobic conditions (Figure S25). The palladium complexes in the triplet state could sensitize the generation of singlet oxygen upon photoirradiation. The efficiency of sensitization was systematically studied by monitoring the UV-vis spectral changes of a well-known singlet oxygen scavenger, 1,5-dihydroxynaphthalene (DHN; $\lambda \sim 340$ nm) in the presence of the photosensitizers (**1-Pd-H₂**, **2-Pd-H₂**, **1-Pd-Pd**, **2-Pd-Pd**, and methylene blue (MB) as a reference) in CH₂Cl₂/MeOH (Figures S19–S24). Singlet oxygen generated *in-situ* can oxidize DHN to juglone upon Xe lamp irradiation (λ_{ex} ; 450–800 nm) (Table 2).^[22] The singlet oxygen quantum yields were calculated using the following equation 1.^[23]

$$\Phi_{\Delta} = \Phi_{\Delta}^{\text{std}} \times (v_i^{\text{std}}/v_i^{\text{std}}), \quad (1)$$

where Φ_{Δ} is the singlet oxygen quantum yield ($\Phi_{\Delta}^{\text{std}} = 0.74$, for MB) in CH₂Cl₂/MeOH, v_i is the initial rate of DHN consumption, and I is the relative number of photons absorbed.^[19] v_i is determined from the slope of the graph $\ln(C_i/C_0)$ in the initial 3 minutes (Figure 6a). As the result, the quantum yields for singlet oxygen generation using the palladium complexes were estimated to be 0.83 (**2-Pd-H₂**) > 0.30 (**1-Pd-Pd**) > 0.27 (**2-Pd-Pd**) > 0.05 (**1-Pd-H₂**) based on the reference value 0.74 (MB) (Table 1). The long-lived triplet excited state of photosensitizer has a higher probability to undergo bimolecular collision with ground state oxygen to generate singlet oxygen.^[2] The huge acceleration in the conversion could be thus related to the triplet-state lifetime of the photosensitizer.

To confirm the singlet oxygen generation in the photosensitization, we conducted the EPR measurements using spin labelling agents, 2,2,6,6-tetramethylpiperidine (TEMP) and 5,5-dimethyl-1-pyrroline-*N*-oxide (DMPO), respectively (Figure 6d). Photoirradiation of an air-saturated toluene solution containing photosensitizer and TEMP resulted in the characteristic three-line EPR spectrum after 3 min. The hyperfine coupling constants, a_N is 16.0 G which can be assigned to TEMPO (TEMP and $^1\Delta_g$ react to form TEMPO).^[24] The TEMPO signal intensity is in the order **2-Pd-H₂** > **1-Pd-Pd** > **2-Pd-Pd** > **1-Pd-H₂**, which is well correlated to the quantum yields of singlet oxygen generation. In contrast, no reaction occurred in the presence of another spin labelling reagent, DMPO, indicating no other reactive

oxygen species (e.g., peroxide, superoxide) are generated under this condition.^[25]

Table 2. Chemical yield of conversion of DHN to juglone in the presence of sensitizer after 60 minutes.

Complex	Chemical yield (%)	% degradation (60 min)
1-Pd-H₂	73	3.1
2-Pd-H₂	83	48.7
1-Pd-Pd	97	2.6
2-Pd-Pd	92	2.7
MB	98	30.1

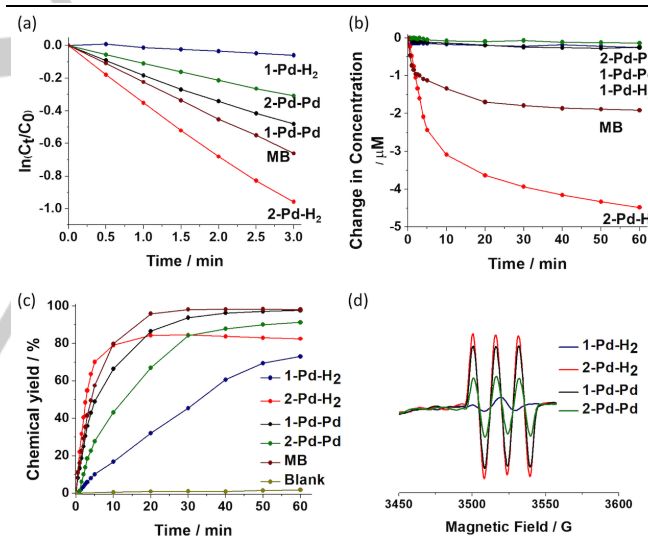


Figure 6. (a) Plot of $\ln(C_i/C_0)$ versus irradiation time for palladium complexes (**1-Pd-H₂**, **2-Pd-H₂**, **1-Pd-Pd**, and **2-Pd-Pd**) and methylene blue (MB). (b) Change in concentrations of the photosensitizers under the irradiation condition. (c) Kinetics of chemical yields of juglone with respect to irradiation time in CH₂Cl₂/MeOH. (d) EPR spectra of the spin trapped species using TEMP in the presence of the palladium complexes in oxygen-saturated toluene solution recorded after 3 minutes of light irradiation (450–800 nm).

Importantly, we tested the durability of the sensitizers under the identical conditions and bis-palladium complexes, **1-Pd-Pd** and **2-Pd-Pd**, were found to be remarkably stable under photoirradiation (Figure 6b, Table 2).^[19] As a result, the actual chemical yields of juglone using the bis-palladium complexes, **1-Pd-Pd** (97%) and **2-Pd-Pd** (92%), were found to be larger than

For internal use, please do not delete. Submitted_Manuscript

FULL PAPER

that of **2-Pd-H₂** (83%) in spite of its higher singlet oxygen quantum yield (Figure 6c). Interestingly, the relatively less effective **1-Pd-H₂** generated juglone gradually but in high yield after 60 min irradiation. In the case of most reactive **2-Pd-H₂**, juglone was rapidly formed but the yield was saturated after 20 min, presumably due to the instability of the complex under the condition used. Based on the above analysis, the photostability of the sensitizers is seen to be one of the most important factors for practical use in applications such as PDT. Without sensitizers the product was obtained only in 2% yield after 60 minutes, indicating the critical role of photosensitizer in this reaction.

Conclusions

In summary, we have synthesized a series of novel triplet photosensitizers based on mono- and bis-palladium calix[6]phyrin complexes, **1-Pd-H₂**, **2-Pd-H₂**, **1-Pd-Pd**, and **2-Pd-Pd**, for singlet oxygen generation. These complexes have broad absorption spectra from the visible to NIR region and appropriate triplet energy (800–1000 nm) and reasonably longer lifetimes (~540 ns) for the sensitization of singlet oxygen generation. The metal number and coordination environment of the complexes play an important role in modulation of the optical properties as well as photostability. Because of the facile synthesis, good singlet oxygen generation capability, and photostability, the current calix[6]phyrin-based photosensitizers would hold promise for applications such as PDT, photo-redox catalysts and so on.

Experimental Section

Materials and Instruments. All reactions were performed in dried vessels under Ar or N₂. Commercially available solvents and reagents were used without further purification unless otherwise mentioned. CH₂Cl₂ was dried by passing through a pad of alumina. Thin-layer chromatography (TLC) was performed on an aluminum sheet coated with silica gel 60 F₂₅₄ (Merck). Preparative separation was performed by silica gel flash column chromatography (KANTO silica gel 60N, spherical, neutral, 40–50 μm) or silica gel gravity column chromatography (KANTO Silica Gel 60N, spherical, neutral, 63–210 μm). ¹H and ¹⁹F NMR spectra were recorded in CDCl₃ solutions on a JEOL ECX500 NMR spectrometer (500 MHz for ¹H and 470 MHz for ¹⁹F). Chemical shifts were reported relative to CDCl₃ (δ = 7.26 ppm) for ¹H in parts per million. Trifluoroacetic acid (0.02% in CDCl₃) was used as an external reference for ¹⁹F (δ = –76.5 ppm). UV–vis–NIR absorption spectra were measured on a Shimadzu UV-3150PC spectrometer. Fluorescence spectra were recorded on a SPEX Fluorolog-3-NIR spectrometer (HORIBA) with an NIR-PMT R5509 photomultiplier tube (Hamamatsu) in a 10 mm quartz fluorescence cuvette. High-resolution mass spectra (HRMS) were obtained in fast atom bombardment (FAB) mode with 3-nitrobenzyl alcohol (NBA) as a matrix on a JEOL LMS-HX-110 spectrometer.

Singlet Oxygen Quantum Yields. Singlet oxygen quantum yields (Φ_Δ) were determined in CH₂Cl₂/MeOH by using 5 mol% of mono- and bis-palladium complexes (**1-Pd-H₂**, **2-Pd-H₂**, **1-Pd-Pd**, and **2-Pd-Pd**) (9 μM) and methylene blue (**MB**) as the reference compound. The singlet oxygen scavenger, dihydroxynaphthalene (DHN, 181 μM) was used as the singlet oxygen scavenger. Alternately, emissions of the singlet oxygen sensitized

by the palladium complexes in O₂ saturated toluene were recorded on an SPEX Fluorolog-3-NIR spectrometer (HORIBA). The solution of a sensitizer with DHN was bubbled with oxygen for 15 minutes to get oxygen saturated solution. Then the solution was irradiated with 450–800 nm light using a bandpass filter and photoirradiation was carried out using a Xe lamp of 300 W.

Time-Resolved Emission Spectroscopy. Time-resolved phosphorescence measurements were performed in the time-correlated single photon counting mode using a NIR-sensitive photomultiplier (Hamamatsu H10330-75). The excitation source was a 532 nm frequency-doubled passive-Q-switched Nd:YAG laser delivering a 1 μJ sub-nanosecond (<0.7 ns) pulse train at a repetition rate of 8 kHz. The sample solutions (toluene solvent) in the cell cuvette were carefully degassed by argon (gas) bubbling with septum.

Theoretical Calculations. DFT calculations were performed with the Gaussian16 program package without symmetry treatment.^[26] Initial structures were based on the X-ray crystal structure of the related compounds. The geometries were fully optimized using Becke's three-parameter hybrid functional combined with the Lee–Yang–Parr correlation functional, denoted as the B3LYP level of DFT, with the 6-31G(d,p), and SDD (for Pd) basis set for all calculations.^[27] Experimental absorption spectra were analyzed by time-dependent DFT (TD-DFT) calculations with the same level. Ground-state geometries were verified by the frequency calculations, where no imaginary frequency was found. For visualization of the optimized geometries and the molecular orbitals, GaussView software was used.

X-ray Crystallography. Single-crystal X-ray structural analyses for **1-Pd-H₂**, **2-Pd-H₂**, **3-Pd-Pd**, and **4-Pd-Pd** were performed on a Saturn diffractometer equipped with a CCD detector (Rigaku) using MoKα (graphite, monochromatized, λ = 0.71069 Å) radiation. The data were corrected for Lorentz, polarization, and absorption effects and refined using the SHELXS-2014/7 program.^[28] All of the positional parameters and thermal parameters of non-hydrogen atoms were refined anisotropically on F² by the full-matrix least-squares method. Hydrogen atoms were placed at calculated positions and refined using a riding model on their corresponding carbon atoms. The crystal-to-detector distance was 45.00 mm.

Synthesis of Precursors. The freebase doubly N-confused calix[6]phyrins (**1-4**) were synthesized by following the procedure reported previously.^[14] Detailed characterization data for **1-Pd-H₂**, **2-Pd-H₂**, **1-Pd-Pd**, and **2-Pd-Pd** is given in *Supporting Information*.

General method for synthesis of mono-palladium complexes (1-Pd-H₂): A mixture of free ligand, **1** (20 mg, 0.015 mmol) and Pd(OAc)₂ salt (3.8 mg, 0.017 mmol) in CH₂Cl₂/MeOH (2:1) was stirred under argon for 2 h under reflux conditions (40 °C). The solvents were removed in vacuo using high vacuum pump. The crude product was purified using silica gel column chromatography with CH₂Cl₂/hexane mixture.

The complex, **2-Pd-H₂** was also synthesized using **2** under the same conditions.

Data for **1-Pd-H₂**: yield = 80% (17.2 mg); ¹H NMR (CDCl₃, ppm): δ 12.90 (s, 1H), 10.59 (s, 1H), 6.65 (d, J = 4.8 Hz, 1H), 6.62 (d, J = 4.8 Hz, 1H), 6.59 (s, 1H), 6.54 (d, J = 4.5 Hz, 1H), 6.48 (d, J = 4.4 Hz, 1H), 6.36 (d, J = 4.3 Hz, 1H), 6.33 (d, J = 4.3 Hz, 1H), 6.19 (d, J = 4.2 Hz, 1H), 5.98 (s, 1H), 5.94 (s, 1H), 3.29 (s, 2H), 2.99 (s, 1H), 2.54 (s, 1H), 2.24 (s, 4H), 1.82 (m, 4H), 1.57 (m, 8H); ¹⁹F NMR (CDCl₃, ppm): δ –136.42 (s), –136.96 (s), –137.24 (s), –137.62 (s), –138.21 (s), –138.69 (s), –138.94 ~ –139.15 (m), –150.99 (d, J = 38.5 Hz), –151.82 (d, J = 34.0 Hz), –152.41 (d, J = 39.5

For internal use, please do not delete. Submitted_Manuscript

FULL PAPER

Hz), -159.33 (s), -160.07 (s), -160.27 (d, $J = 25.9$ Hz), -160.70 (d, $J = 64.1$ Hz), -160.99 (s); HRMS (FAB⁺): $m/z = 1371.1481$ (found), 1371.1482 (Calcd for C₆₄H₃₃F₂₀N₆Pd), error -0.1 ppm.

Data for **2-Pd-H₂**: yield = 75 % (16.1 mg); ¹H NMR (CDCl₃, ppm): δ 10.26 (s, 1H), 6.65 (d, $J = 4.6$ Hz, 1H), 6.50 (d, $J = 4.6$ Hz, 1H), 6.41 (d, $J = 4.6$ Hz, 1H), 6.36 (d, $J = 4.5$ Hz, 1H), 5.93 (s, 1H), 3.38 (s, 1H), 2.88 (s, 1H), 2.27 (s, 1H), 2.21 (s, 1H), 1.83 (s, 1H), 1.62 (m, 5H); ¹⁹F NMR (CDCl₃, ppm): δ -136.69 (s), -137.28 (s), -138.57 (d, $J = 23.9$ Hz), -138.94 (s), -151.13 (s), -152.32 (d, $J = 38.7$ Hz), -159.82 (s), -160.29 (s), -160.58 (s), -160.90 (s); HRMS (FAB⁺): $m/z = 1371.1484$ (found), 1371.1482 (Calcd for C₆₄H₃₃F₂₀N₆Pd), error + 0.1 ppm.

General method for synthesis of bis-palladium complexes (1-Pd-Pd): A mixture of free ligand **1** (20 mg, 0.015 mmol) and Pd(OAc)₂ (11.4 mg, 0.052 mmol) in CH₂Cl₂/MeOH (2:1) was stirred under argon for 12 h under reflux conditions (40 °C). The solvents were removed *in vacuo* using high vacuum pump. The crude product was purified using silica gel column chromatography with CH₂Cl₂/hexane mixture.

Data for **1-Pd-Pd**: yield = 60% (14 mg); ¹H NMR (CDCl₃, ppm): δ 6.59 (d, $J = 4.5$ Hz, 1H), 6.55 (d, $J = 4.7$ Hz, 1H), 6.48 (d, $J = 4.6$ Hz, 1H), 6.41 (d, $J = 4.4$ Hz, 1H), 5.90 (s, 1H), 3.26 (s, 1H), 3.06 (s, 1H), 2.26 (m, 2H), 1.83 (m, 2H), 1.58 (m, 4H); ¹⁹F NMR (CDCl₃, ppm): δ -137.37 (s), -138.72 (d, $J = 21.9$ Hz), -139.13 (d, $J = 24.7$ Hz), -151.67 (d, $J = 57.9$ Hz), -159.73 (s), -160.08 (s), -160.61 (s), -160.93 (s); HRMS (FAB⁺): $m/z = 1474.0290$ (found), 1474.0282 (Calcd for C₆₄H₃₀F₂₀N₆Pd₂), error + 0.5 ppm.

Data for **2-Pd-Pd**: yield = 71% (16.5 mg); ¹H NMR (CDCl₃, ppm): δ 6.64 (d, $J = 4.7$ Hz, 1H), 6.48 (t, $J = 5.2$ Hz, 2H), 6.38 (d, $J = 4.4$ Hz, 1H), 5.93 (s, 1H), 3.21 (s, 1H), 3.09 (s, 1H), 2.25 (m, 2H), 1.80 (s, 2H), 1.55 (m, 4H); ¹⁹F NMR (CDCl₃, ppm): δ -137.35 (d, $J = 23.6$ Hz), -138.71 ~ -139.28 (m), -151.65 (d, $J = 37.5$ Hz), -159.54 ~ -160.14 (m), -160.77 (d, $J = 87.8$ Hz); HRMS (FAB⁺): $m/z = 1474.0285$ (found), 1474.0282 (Calcd for C₆₄H₃₀F₂₀N₆Pd₂), error + 0.2 ppm.

Data for **3-Pd-Pd**: ¹H NMR (CDCl₃, ppm): δ 6.52 (m, 4H), 6.48 (d, $J = 4.7$ Hz, 2H), 6.40 (d, $J = 4.4$ Hz, 2H), 5.94 (s, 2H), 2.27 (s, 6H), 1.76 (s, 6H); ¹⁹F NMR (CDCl₃, ppm): δ -137.49 (s), -137.55 (d, $J = 22.4$ Hz), -138.88 (d, $J = 22.9$ Hz), -139.36 (d, $J = 22.4$ Hz), -139.40 ~ -139.55 (m), -151.52 (s), -151.57 (s), -151.61 (s), -151.68 (s), -151.74 (d, $J = 19.0$ Hz), -159.72 (t, $J = 22.7$ Hz), -160.06 (t, $J = 18.8$ Hz), -160.70 (s), -160.75 (s), -160.77 (d, $J = 21.5$ Hz), -160.72 ~ -161.52 (m); HRMS (FAB⁺): $m/z = 1393.9684$ (found), 1393.9656 (Calcd for C₅₈H₂₂F₂₀N₆Pd₂), error + 2.0 ppm.

Data for **4-Pd-Pd**: ¹H NMR (CDCl₃, ppm): δ 6.60 (m, 2H), 6.47 (d, $J = 4.6$ Hz, 2H), 6.42 (m, 2H), 6.37 (d, $J = 4.4$ Hz, 2H), 5.97 (s, 2H), 2.27 (d, $J = 10.1$ Hz, 6H), 1.75 (d, $J = 13.9$ Hz, 6H); ¹⁹F NMR (CDCl₃, ppm): δ -137.53 (m, 26.8 Hz), -138.95 (d, $J = 28.3$ Hz), -139.35 (d, $J = 28.8$ Hz), -151.65 (t, $J = 22.9$ Hz), -159.79 (t, $J = 21.7$ Hz), -159.99 (t, $J = 21.8$ Hz), -160.83 (t, $J = 21.5$ Hz), -161.04 (t, $J = 21.8$ Hz); HRMS (FAB⁺): $m/z = 1393.9658$ (found), 1393.9656 (Calcd for C₅₈H₂₂F₂₀N₆Pd₂), error + 0.1 ppm.

Acknowledgements

The present work was supported by Grants-in-Aid (JP15K13646 to H.F.; JP16K05700 and JP17H05377 to M.I.; JP17H02773 and JP18K19029 to S.F.) from the Japan Society for the Promotion of Science (JSPS).

Keywords: Triplet Photosensitizer • Palladium N-confused calix[6]phyrin • Singlet oxygen • Photostability

- [1] a) J. J. Liang, C. L. Gu, M. L. Kacher, C. S. Foote, *J. Am. Chem. Soc.* **1983**, *105*, 4717–4721; b) J. L. Ravanat, P. Di Mascio, G. R. Martinez, M. H. Medeiros, J. Cadet, *J. Biol. Chem.* **2000**, *275*, 40601–40604; c) M. C. DeRosa, R. J. Crutchley, *Coord. Chem. Rev.* **2002**, *233–234*, 351–371; d) P. R. Ogilby, *Chem. Soc. Rev.* **2010**, *39*, 3181–3209.
- [2] C. Schweitzer, R. Schmidt, *Chem. Rev.* **2003**, *103*, 1685–1758.
- [3] a) D. E. J. G. J. Dolmans, D. Fukumura, R. K. Jain, *Nat. Rev. Cancer* **2003**, *3*, 380–387; b) C. A. Robertson, D. H. Evans, H. Abrahamse, *J. Photochem. Photobiol. B* **2009**, *96*, 1–8; c) M. C. Issa, M. Manela-Azulay, *An. Bras. Dermatol.* **2010**, *85*, 501–511.
- [4] a) C. Huo, H. Zhang, H. Zhang, H. Zhang, B. Yang, P. Zhang, Y. Wang, *Inorg. Chem.* **2006**, *45*, 4735–4742; b) X. Jiang, J. Peng, J. Wang, X. Guo, D. Zhao, Y. Ma, *ACS App. Mater. Interfaces* **2016**, *8*, 3591–3600.
- [5] a) O. Suchard, R. Kane, B. J. Roe, E. Zimmermann, C. Jung, P. A. Waske, J. Mattay, M. Oelgemöller, *Tetrahedron* **2006**, *62*, 1467–1473; b) L. Huang, J. Zhao, S. Guo, C. Zhang, J. Ma, *J. Org. Chem.* **2013**, *78*, 5627–5637; c) W.-P. To, Y. Liu, T.-C. Lau, C.-M. Che, *Chem. Eur. J.* **2013**, *19*, 5654–5664.
- [6] a) X. Cui, J. Zhao, P. Yang, J. Sun, *Chem. Comm.* **2013**, *49*, 10221–10223; b) T. N. Singh-Rachford, F. N. Castellano, *Coord. Chem. Rev.* **2010**, *254*, 2560–2573.
- [7] a) T. Yogo, Y. Urano, Y. Ishitsuka, F. Maniwa, T. Nagano, *J. Am. Chem. Soc.* **2005**, *127*, 12162–12163; b) W. Wu, H. Guo, W. Wu, S. Ji, J. Zhao, *J. Org. Chem.* **2011**, *76*, 7056–7064.
- [8] a) F. Heinemann, J. Karges, G. Gasser, *Acc. Chem. Res.* **2017**, *50*, 2727–2736; b) D. N. Kozhevnikov, V. N. Kozhevnikov, M. Z. Shafikov, A. M. Prokhorov, D. W. Bruce, J. A. Gareth Williams, *Inorg. Chem.* **2011**, *50*, 3804–3815; c) X. Wang, S. Goeb, Z. Ji, N. A. Pogulaichenko, F. N. Castellano, *Inorg. Chem.* **2011**, *50*, 705–707; d) T. Sajoto, P. I. Djurovich, A. B. Tamayo, J. Oxgaard, W. A. Goddard, M. E. Thompson, *J. Am. Chem. Soc.* **2009**, *131*, 9813–9822; e) J. I. Goldsmith, W. R. Hudson, M. S. Lowry, T. H. Anderson, S. Bernhard, *J. Am. Chem. Soc.* **2005**, *127*, 7502–7510.
- [9] a) Y. Che, W. Yang, G. Tang, F. Dumoulin, J. Zhao, L. Liu, Ü. İşci, *J. Mater. Chem. C* **2018**, *6*, 5785–5793; b) M. Ethirajan, Y. Chen, P. Joshi, R. K. Pandey, *Chem. Soc. Rev.* **2011**, *40*, 340–362; c) T. N. Singh-Rachford, F. N. Castellano, *J. Phys. Chem. A* **2008**, *112*, 3550–3556.
- [10] a) A. Srinivasan, H. Furuta, *Acc. Chem. Res.* **2005**, *38*, 10–20; b) J. R. Sommer, A. H. Shelton, A. Parthasarathy, I. Ghiviriga, J. R. Reynolds, K. S. Schanze, *Chem. Mater.* **2011**, *23*, 5296–5304; c) M. Toganoh, H. Furuta, *Chem. Comm.* **2012**, *48*, 937–954; d) V. V. Roznyatovskiy, C.-H. Lee, J. L. Sessler, *Chem. Soc. Rev.* **2013**, *42*, 1921–1933; e) T. Chatterjee, V. S. Shetti, R. Sharma, M. Ravikanth, *Chem. Rev.* **2017**, *117*, 3254–3328; f) S. Hiroto, Y. Miyake, H. Shinokubo, *Chem. Rev.* **2017**, *117*, 2910–3043.
- [11] a) A. Singhal, in *Top Curr Chem*, **2018**, *376*, 21; b) J. L. Sessler, R. S. Zimmerman, C. Bucher, V. Král, B. Andrioletti, *Pure Appl. Chem.* **2001**, *73*, 1041–1057; c) A. C. Y. Tay, B. J. Frogley, D. C. Ware, P. J. Brothers, *Dalton Trans.* **2018**, *47*, 3388–3399.
- [12] a) K. Araki, F. N. Engemann, I. Mayer, H. E. Toma, M. S. Baptista, H. Maeda, A. Osuka, H. Furuta, *Chem. Lett.* **2003**, *32*, 244–245; b) K. Araki, F. N. Engemann, I. Mayer, H. E. Toma, M. S. Baptista, H. Maeda, A. Osuka, H. Furuta, *J. Photochem. Photobiol. A* **2004**, *163*, 403–411.
- [13] a) H. Furuta, T. Ishizuka, A. Osuka, Y. Uwatoko, Y.; Ishikawa, *Angew. Chem. Int. Ed.* **2001**, *40*, 2323–2325; b) H. Furuta, T. Ishizuka, A. Osuka, *Inorg. Chem. Commun.* **2003**, *6*, 398–401; c) P. Pushpanandan, Y. K. Maurya, T. Omagari, R. Hirose, M. Ishida, S. Mori, Y. Yasutake, S. Fukatsu, J. Mack, T. Nyokong, H. Furuta, *Inorg. Chem.* **2017**, *56*, 12572–12580.
- [14] D.-H. Won, M. Toganoh, Y. Terada, S. Fukatsu, H. Uno, H. Furuta, *Angew. Chem.* **2008**, *47*, 5438–5441.

For internal use, please do not delete. Submitted Manuscript

FULL PAPER

- [15] a) M. Gouterman, F. P. Schwarz, P. D. Smith, D. Dolphin, *J. Chem. Phys.* **1973**, *59*, 676–690; b) S. M. Borisov, G. Zenkl, I. Klimant, *ACS Appl. Mater. Interfaces* **2010**, *2*, 366–374; c) S. Drouet, C. O. Paul-Roth, V. Fattori, M. Cocchi, J. A. G. Williams, *New J. Chem.* **2011**, *35*, 438–444; d) E. I. G. Azenha, A. C. Serra, M. Pineiro, M. M. Pereira, J. Seixas de Melo, L. G. Arnaut, S. J. Formosinho, A. M. d'A. R. Gonsalves, *Chem. Phys.* **2002**, *280*, 177–190.
- [16] S. Gokulnath, K. Nishimura, M. Toganoh, S. Mori, H. Furuta, *Angew. Chem.* **2013**, *52*, 6940–6943.
- [17] a) H. Furuta, N. Kubo, H. Maeda, T. Ishizuka, A. Osuka, H. Nanami, T. Ogawa, *Inorg. Chem.* **2000**, *39*, 5424–5425; b) H. Furuta, H. Maeda, A. Osuka, M. Yasutake, T. Shinmyozu, Y. Ishikawa, *Chem. Comm.* **2000**, 1143–1144.
- [18] a) J. H. Kwon, T. K. Ahn, M.-C. Yoon, D. Y. Kim, M. K. Koh, D. Kim, H. Furuta, M. Suzuki, A. Osuka, *J. Phys. Chem. B* **2006**, *110*, 11683–11690; b) S. Gokulnath, K. Yamaguchi, M. Toganoh, S. Mori, H. Uno, H. Furuta, *Angew. Chem.* **2011**, *50*, 2302–2306.
- [19] S.-y. Takizawa, R. Aboshi, S. Murata, *Photochem. Photobiol. Sci.* **2011**, *10*, 895–903
- [20] B. Dolenský, J. Kroulík, V. Král, J. L. Sessler, H. Dvořáková, P. Bouř, M. Bernátková, C. Bucher, V. Lynch, *J. Am. Chem. Soc.* **2004**, *126*, 13714–13722.
- [21] J. V. Caspar, E. M. Kober, B. P. Sullivan, T. J. Meyer, *J. Am. Chem. Soc.* **1982**, *104*, 630–632.
- [22] D. Murtinho, M. Pineiro, M. M. Pereira, A. M. d'A. R. Gonsalves, L. G. Arnaut, M. G. Miguel, H. D. Burrows, *Perkin Trans. 2* **2000**, 2441–2447.
- [23] A. Ogunsipe, T. Nyokong, *J. Mol. Struct.* **2004**, *689*, 89–97.
- [24] a) Y. Lion, M. Delmelle, A. Van De Vorst, *Nature* **1976**, *263*, 442–443; b) J. Moan, E. Wold, *Nature* **1979**, *279*, 450–451.
- [25] J. Wang, Y. Hou, W. Lei, Q. Zhou, C. Li, B. Zhang, X. Wang, *ChemPhysChem* **2012**, *13*, 2739–2747.
- [26] M. J. Frisch, G. W. Trucks, H. B. Schlegel, G. E. Scuseria, M. A. Robb, J. R. Cheeseman, G. Scalmani, V. Barone, G. A. Petersson, H. Nakatsuji, X. Li, M. Caricato, A. V. Marenich, J. Bloino, B. G. Janesko, R. Gomperts, B. Mennucci, H. P. Hratchian, J. V. Ortiz, A. F. Izmaylov, J. L. Sonnenberg, Williams, F. Ding, F. Lipparini, F. Egidi, J. Goings, B. Peng, A. Petrone, T. Henderson, D. Ranasinghe, V. G. Zakrzewski, J. Gao, N. Rega, G. Zheng, W. Liang, M. Hada, M. Ehara, K. Toyota, R. Fukuda, J. Hasegawa, M. Ishida, T. Nakajima, Y. Honda, O. Kitao, H. Nakai, T. Vreven, K. Throssell, J. A. Montgomery Jr., J. E. Peralta, F. Ogliaro, M. J. Bearpark, J. J. Heyd, E. N. Brothers, K. N. Kudin, V. N. Staroverov, T. A. Keith, R. Kobayashi, J. Normand, K. Raghavachari, A. P. Rendell, J. C. Burant, S. S. Iyengar, J. Tomasi, M. Cossi, J. M. Millam, M. Klene, C. Adamo, R. Cammi, J. W. Ochterski, R. L. Martin, K. Morokuma, O. Farkas, J. B. Foresman, D. J. Fox, Wallingford, CT, **2016**.
- [27] a) A. D. Becke, *J. Chem. Phys.* **1993**, *98*, 5648–5652; b) P. J. Stephens, F. J. Devlin, C. F. Chabalowski, M. J. Frisch, *J. Phys. Chem.* **1994**, *98*, 11623–11627.
- [28] a) G. M. Sheldrick, *Acta. Crystallogr. A* **2008**, *64*, 112–122. b) G. M. Sheldrick, *Acta. Crystallogr. A* **2015**, *71*, 3–8. c) G. M. Sheldrick, *Acta. Crystallogr. C* **2015**, *71*, 3–8.